Research Journal of Applied Sciences 12 (2): 242-253, 2017
ISSN: 1815-932X

Geochemical Characterization of Trachytic Rocks at Gabal Abu Hibban, Central Eastern Desert, Egypt and Their Suitability as a Flux in the Ceramic Industry

[1]B.N.A. Shalaby, [2]M.S. El-Maghraby, [1]A.O. Mashaly and [1]A.K.A. Salem
[1]Department of Geology, National Research Centre, Cairo, Egypt
[2]Department of Ceramics, Refractories and Building Materials,
National Research Centre, Cairo, Egypt

Abstract: Gabal Abu Hibban, Southwest of Port Qusseir is represented mainly by trachytic rocks in the form of lava flows, sheets, dykes and sills. Petrographically, these rocks are composed mainly of sanidine and albite phenocyrsts with less frequent aegerine and aegerine augite in addition to sodic amphibole, zircon and biotite. The amount of quartz varies greatly from 0% up to 12% of the rock volume. Geochemically, trachytes from Gabal Abu Hibban exhibited a remarked alkaline-peralkaline, meta-aluminous nature as revealed from agpaitic index, feldspathoid silica saturation index, modified alkali-lime index and the aluminum saturation index. Based on CIPW norms, Abu Hibban Trachytes (AHT) comprise nepheline normative and quartz normative varieties. These trachytes were derived from more basic alkali rich magma had undergone fractionation giving rise to more fractionated trachytic rocks. Variation diagrams and elemental ratios revealed a combined role of fractional crystallization and crustal contamination affected the differentiation trends between nepheline normative trachytes and quartz normative trachytes. Abu Hibban Trachytes (AHT) erupted within continental plate, characterized by enrichment in immobile elements; Zr, Y, P and Ti and depletion in mobile elements; Sr, Ba, Rb and K with respect to that formed within oceanic plate. Such variations between the two suites reflect the role of the subcontinental lithosphere in the continental rift zones. Assessment of the possibility of utilization of nepheline as well as quartz trachyte as a flux comparable with the widely used K-feldspar was performed based on the chemical and mineral compositions of the trachytes. The melting behaviour of the trachyte as well as the K-feldspar cone samples were tested after firing for 1 h at 1100 and 1200°C. Solid-phase composition of the samples was semi-quantitatively determined using XRD. Nepheline as well as quartz normative trachytes exhibited melting point lesser than K-feldspar and a completely liquid phase was formed on firing at 1200°C, this indicates that the present trachyte can partially or completely replace K-feldspar in the ceramic mixture as a flux.

Key words: Trachyte, ceramic industry, alkaline rocks, anorogenic, geochemistry

INTRODUCTION

The phanerozoic volcanism in Egypt initialized after the ceasing of the Pan-African Orogeny (950-550 Ma) and erupted through seven episodes of intraplate magmatisms; paleozoic magmatism, early triassic magmatism, late Jurassic magmatism, early cretaceous magmatism, late cretaceous magmatism, tertiary magmatism and oligocene-miocene magmatism. These volcanisms were mostly erupted in the Eastern Desert of Egypt in the form of ring complexes, volcanic plugs, sills, sheets and dykes and represented by alkali (transitional) basalts, trachytes (phonolites) and alkaline to peralkaline rhyolites in addition to their plutonic equivalents. The composition of their parental melts varies from silica undersaturated (Ne-normative) to silica saturated (olivine normative) to silica oversaturated (Quartz normative) and on further fractionation the composition of their parental melts deviates toward alkali rhyolites (comendite or pentellerite) due to the processes of Assimilation Fractional Crystallization (ACF) crustal contamination or magma mixing, especially at the later stages of fractionation by Hashad *et al.* (1978), Meneisy (1986), Hashad (1994), Moghazi *et al.* (1997), Mohamed (1998, 2001), Aly and Shalaby (2001), Gharib *et al.*, 2012).

Akaad and El-Ramly distinguished the alkaline rocks in Egypt under three main groups, namely "Alkaline granites", "undersaturated syenites and associated types" and "the late alkaline volcanic suite" which include volcanic plugs, ring dykes and dykes. Gharib *et al.* (2012) studied the trachytic plugs at Um Shaghir and Um Khors West of Qusseir area, Egypt and concluded that these Paleozoic alkaline volcanics are represented by

Corresponding Author: B.N.A. Shalaby, Department of Geology, National Research Centre, Cairo, Egypt

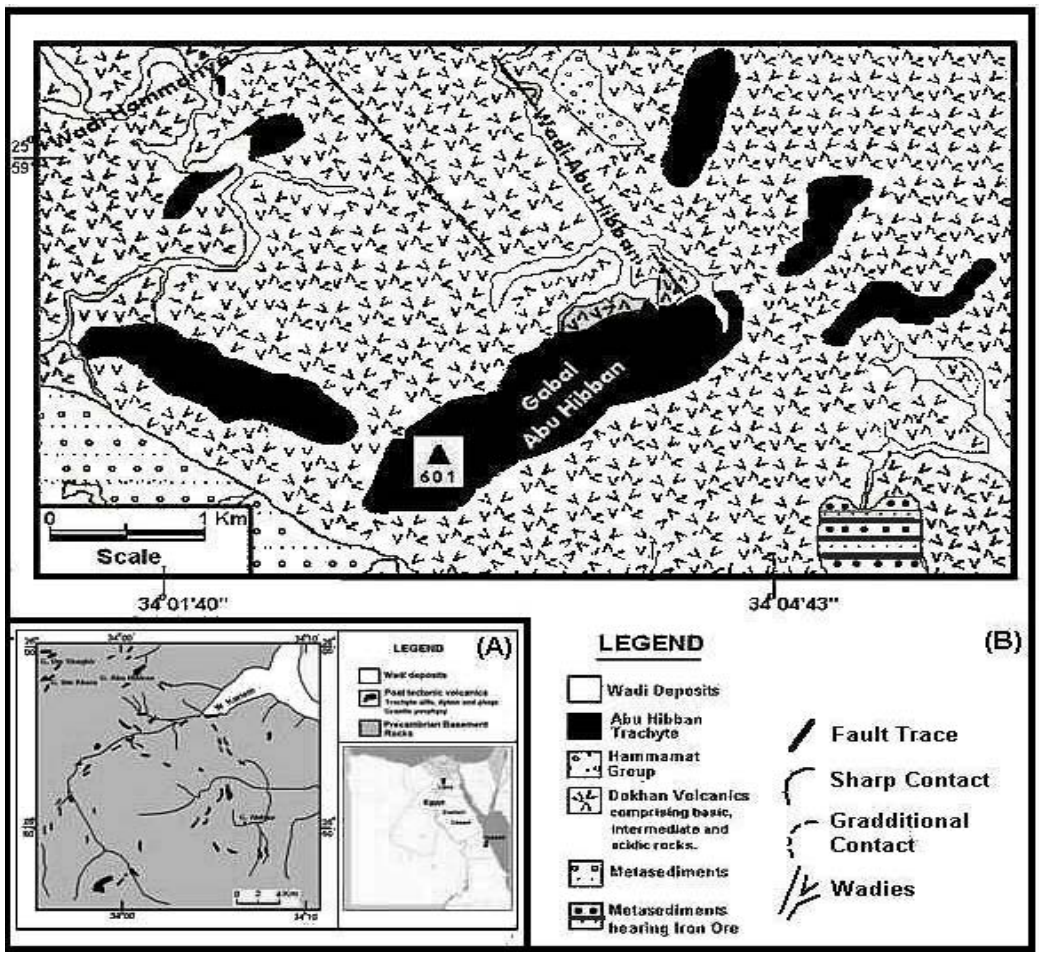

Fig. 1: a) Location map for the alkaline suites west of port Qusseir and b) Geological map of Gabal Abu Hibban trachytic rocks

highly fractionated quartz trachyte evolved from magmatism of extensional tectonic regime. Many exposures of alkaline volcanics encountered in the West and Southwest area from Port Qusseir, the main localities are Gabal Abu Hibban, Wadi Kariem trachytic plugs, Gabal Um Shaghir, Gabal Um Khors, Gabal Atshan area, etc., these rocks described by Dawood *et al.* (2004) as post tectonic volcanics comprising trachytic sills, dykes and plugs, granite porphyry in addition to less common basic rocks (Fig. 1).

Field observations: Gabal Abu Hibban alkaline extrusions are located to the Southwest of Port Qusseir, covering an area of about 21 km^2. The main extrusion is at Gabal Abu Hibban (Alt. 601 m above sea level, Lat. 25°57'51"W and Long 34°02'44"N) covers an area of about 2 km^2, the extrusion is represented mainly by trachytic rocks with a lesser amount of carbonate rich volcanic rocks in the form of lava flows, sheets, dykes and sills.

The main trend of dykes and sills is NE-SW direction, reaching up to 3 km in length, cutting through the surrounding older basement rocks. The alkaline lava flows usually occupy, uncomformably, the summits of the hilly basement rocks of Proterozoic age. The country rocks comprise metasediments and subduction related volcanics, mainly Dokhan Volcanics which include basalt andesite, dacite and rhyolite (Fig. 1b). The trachytic rocks vary in colour from grayish brown to reddish brown they are fine grained, hard, massive and more resistant than the surrounding country rocks.

Utilizing of alkaline rocks as a flux in ceramic industries: A flux is a material that lowers the fusion temperature of the mixture at which it added. These materials are rich in alkalies and alkali earths the higher the alkali content the more effective it will be as fluxing agent. The flux must be low in impurities as titania and iron oxides (Ryan and Radford, 1987).

Feldspathoids minerals are rich in potassium and sodium alkalies than feldspars due to their crystallization after feldspar from magma enriched in alkalies and deficient in silica, yielding nepheline and leucite (Na, K Al SiO_4). Nepheline (Na>K Al SiO_4) with a frequent Na:K ratio of ~3:1, is the most common feldspathoid minerals. Its alkali content is substantially higher than alkali feldspars due to the substitution of the tetrahedral Si by Al up to 1:1 ratio with positive charge alkali, Na, K ions.

The eutectic between nepheline and albite phases exists at ca. 1060°C. Among nepheline raw materials, nepheline syenites and trachytes are the most important rocks containing major nepheline mineral. These rocks can be applied for the manufacture of a wide variety of ceramics as a vitrifying agent which contributes in developing a glassy phase to bind other constituents and gives strength to the ware, nepheline syenite is an essential constituent in ceramics and glass raw materials as a flux and as a source of alumina. The natural nepheline syenite rocks contain some undesired minerals which are usually eliminated or reduced to the allowable limits by beneficiation (Gaied and Gallala, 2015).

The effect of the addition of nepheline syenite on sanitary ware porcelain was investigated and confirmed that, the presence of nepheline-syenite strongly enhances the sintering behavior (Esposito *et al*., 2005; Kunduraci and Aydin, 2015).

The scope of the present research is to study the geochemical characteristics of AHT, based on their mineralogical and chemical classification the nature of their parent magma from which they were derived their fractionation trends and their tectonic setting. The scope is also aiming to study the possibility of utilizing the present AHT in ceramic industry as a flux comparable with the K-feldspars.

MATERIALS AND METHODS

Eleven representative trachyte samples from Gabal Abu Hibban, central Eastern Desert of Egypt were selected for major oxides and trace elements chemical analyses (Table 1). For the purpose of utilization of nepheline as well as quartz trachyte as flux in ceramic industry comparable with the K-feldspars, aindustry comparable with the K-feldspars, a representative average

Table 1: Chemical analyses and CIPW norms of Abu Hibban trachyte rocks

	Ne-trachyte							Qz-trachyte					
Variables	1	2	3	4	5	6	Average	7	8	9	10	11	Average
Major oxide (wt.%)													
SiO_2	60.31	61.44	62.00	62.29	62.31	62.92	61.88	66.20	67.50	67.90	68.70	69.72	68.00
Al_2O_3	17.62	17.07	17.83	18.76	17.90	16.51	17.62	15.36	14.32	15.11	14.07	14.12	14.60
Fe_2O_3*	04.35	4.75	4.85	4.12	4.85	05.56	4.75	04.06	03.53	3.50	3.81	3.15	3.61
TiO_2	00.11	0.09	0.08	0.07	0.08	00.24	0.11	00.07	00.14	0.12	0.09	0.08	0.10
MnO	00.24	0.23	0.21	0.19	0.23	00.20	0.22	00.12	00.05	0.05	0.07	0.06	0.07
CaO	01.01	0.95	1.08	0.99	0.93	01.15	1.02	00.98	00.83	0.87	0.91	0.85	0.89
MgO	00.13	0.21	0.19	0.11	0.11	00.15	0.15	00.17	00.43	0.32	0.45	0.31	0.34
Na_2O	08.86	7.14	7.99	8.49	8.39	07.37	8.04	07.25	06.17	6.93	6.86	6.13	6.67
K_2O	05.98	5.16	5.18	5.34	5.10	05.34	5.35	03.48	03.73	3.82	3.51	3.17	3.54
P_2O_5	00.02	0.02	0.03	0.02	0.03	00.05	0.03	00.06	00.02	0.02	0.04	0.07	0.04
H_2O	01.18	1.70	0.36	0.17	0.14	00.26	0.63	00.83	01.09	0.81	0.69	0.98	0.88
CO_2	00.15	0.19	0.18	0.11	0.08	00.44	0.19	00.64	00.30	0.48	0.37	0.65	0.49
Total	99.96	98.95	99.98	100.66	100.15	100.19	99.98	99.22	98.11	99.93	99.57	99.29	99.22
Trace element (ppm)													
Rb	139.00	131.00	134.00	197.00	184.00	112.00	149.50	204.00	186.00	190.00	187.00	168.00	187.00
Sr	66.00	57.00	57.00	98.00	90.00	058.00	71.00	50.00	38.00	39.00	38.00	32.00	39.40
Ba	67.00	70.00	41.00	57.00	63.00	046.00	57.33	34.00	24.00	26.00	22.00	22.00	25.60
Cr	3.00	2.00	3.00	03.00	3.00	005.00	3.17	2.00	2.00	2.00	2.00	2.00	2.00
Ni	3.00	3.00	3.00	3.00	3.00	003.00	3.00	6.00	5.00	7.00	4.00	3.00	5.00
Co	4.00	4.00	6.00	5.00	5.00	005.00	4.83	11.00	11.00	11.00	10.00	8.00	10.20
Cu	3.00	3.00	4.00	3.00	3.00	003.00	3.17	5.00	7.00	9.00	8.00	7.00	7.20
Zn	159.00	205.00	191.00	211.00	218.00	141.00	187.50	211.00	179.00	165.00	168.00	134.00	171.40
Pb	14.00	17.00	13.00	14.00	16.00	10.00	14.00	14.00	15.00	15.00	16.00	16.00	15.20
Zr	1322.00	1379.00	1298.00	1473.00	1499.00	656.00	1271.20	2080.00	2873.00	2439.00	2489.00	1935.00	2363.20
Nb	279.00	246.00	271.00	302.00	315.00	211.00	270.67	464.00	551.00	572.00	566.00	496.00	529.80
Th	25.00	26.00	19.00	021.00	30.00	16.00	22.83	58.00	52.00	49.00	41.00	44.00	048.80
Y	79.00	80.00	73.00	85.00	90.00	68.00	79.17	157.00	198.00	199.00	187.00	148.00	177.80
U	-	-	5.00	-	13.00	6.00	8.00	9.00	8.00	9.00	8.00	-	8.50
La	139.00	148.00	163.00	178.00	186.00	150.00	160.67	266.00	308.00	297.00	317.00	261.00	289.80
Ce	204.00	193.00	84.00	205.00	284.00	221.00	198.50	343.00	456.00	437.00	396.00	337.00	393.80
CIPW norm													
Cc	0.34	0.43	0.41	0.25	0.18	1.00	0.44	01.46	00.68	1.08	0.84	1.35	1.08
Ap	0.05	0.05	0.07	0.05	0.07	0.12	0.07	00.14	00.05	0.05	0.09	0.16	0.10
Il	0.21	0.17	0.15	0.13	0.15	0.46	0.21	00.13	00.27	0.23	0.17	0.15	0.19
Or	35.41	30.57	30.61	31.63	30.21	31.63	31.68	20.57	22.04	22.57	20.74	18.73	20.93
Ab	39.42	55.62	50.76	47.87	48.84	53.43	49.32	59.63	52.57	56.45	52.83	51.21	54.54

Table 1: Continue

	Ne-trachyte							Qz-trachyte					
Variabls	1	2	3	4	5	6	Average	7	8	9	10	11	Average
Na-metasilicate	2.10	0.00	0.00	0.00	0.00	0.00	2.10	0.00	0.00	0.00	0.00	0.00	0.00
Aeg	6.31	1.24	4.17	4.53	6.51	6.38	4.86	1.51	0.00	1.93	4.60	0.00	1.61
An	0.00	0.00	0.00	0.00	0.00	0.00	0.00	0.00	0.00	0.00	0.00	0.00	0.00
Cor	0.00	0.00	0.00	0.00	0.00	0.00	0.00	0.00	0.00	0.00	0.00	0.73	0.15
Mt	0.00	2.83	1.42	0.72	0.25	0.83	1.01	2.19	2.55	1.64	0.47	2.29	1.83
Di	3.47	3.07	3.53	3.60	3.46	2.29	3.24	0.37	1.45	0.98	1.64	0.00	0.89
Hyp	0.00	0.00	0.00	0.00	0.00	0.00	0.00	2.82	2.00	2.37	3.49	2.33	2.60
Ol	2.10	1.48	1.94	1.53	2.36	2.90	2.05	0.00	0.00	0.00	0.00	0.00	0.00
Ne	9.21	1.83	6.56	9.20	8.00	0.92	5.95	0.00	0.00	0.00	0.00	0.00	0.00
Qz	0.00	0.00	0.00	0.00	0.00	0.00	0.00	9.58	15.41	11.80	14.02	21.21	14.40
Total	98.62	97.29	99.62	99.51	100.03	99.96	99.17	98.40	97.02	99.10	98.89	98.16	98.31

Table 2: Chemical analyses of the prepared average AHT and raw K-feldspar in weight (%)

Variables	SiO_2	Al_2O_3	Fe_2O_3*	TiO_2	MnO	CaO	MgO	Na_2O	K_2O	P_2O_5	H_2O	CO_2	Total
K-feldspar	75.05	11.96	1.81	0.19	0.03	0.75	0.26	3.31	6.14	0.05	0.01	0.00	99.56
Average AHT	65.40	16.21	4.05	0.10	0.11	0.91	0.26	7.50	4.62	0.03	0.46	0.29	99.94

*Total iron as ferric oxide

sample of AHT was prepared by mixing the investigated quartz and nepheline normative trachytes together in 1:1 weight ratio, grounded into powders with 100 μm particles. Using the raw K-feldspar one batch were designed to contain powder fraction of fine <100 μm. The two prepared batches of trachyte and K-feldspar were mixed well with 5% solution of 2% PVA as binder, hand-shaped as cone samples with 50 mm height and then dried for 24 h at 110°C. The melting behaviour of the representative average trachyte as well as the K-feldspar cone samples was followed after firing for 1 h at temperature 1100 and 1200°C. The solid-phase composition of the trachyte and K-feldspar cone samples fired at 1100 and 1200°C was semi-quantitatively determined by using XRD. The chemical analyses of the two prepared batches of average AHT and K-feldspar are shown in Table 2. The whole rock chemical analyses of the selected AHT samples as well as the two prepared batches of average AHT and K-feldspar were carried out in Spain at Faculty of Geology, Barcelona University by using Philips PW, 1400 computerized X-ray fluorescence spectrometer.

RESULTS AND DISCUSSION

Petrography: The studied trachytic rocks are fine grained, dark grayish brown to reddish brown in colour. They are composed mainly of sanidine and albite with less frequent aegerine and aegerine augite as phenocyrsts in addition to sodic amphibole, zircon and biotite. The amount of quartz varies greatly from 0-12% of the rock volume. Nepheline is not recognized as phenocrysts in the silica deficient varieties. The secondary minerals are mainly iron oxides, epidote and carbonates. Kaolinization and sericitization are the main alteration processes affected the feldspar minerals. The rocks exhibit a pronounced porphyritic nature with phenocrysts forming up to 20% of the rock while the mafic minerals represent <10% of the rock volume. The size of the phenocrysts varies from 0.1-6 mm in length and from 0.05-0.5 mm in width. The quenched groundmass is microcrystalline to cryptocrystalline, exhibits flow or directive texture as the feldspar laths attain a preferred orientation with the flow of the groundmass (Fig. 2). The feldspar and quartz phenocrysts are usually corroded and invaded by the surrounding groundmass (Fig. 3).

Geochemical characteristics: The studied trachytic rocks display SiO_2 contents range from 60.31-69.72% and define two suites; an oversaturated suite with trachytes contain 14.40% normative quartz in average and an undersaturated suite with trachytes contain average of 5.95% normative nepheline. Both types attain an alkali nature as the content of normative anorthite is zero in all samples and the chief feldspar composition is alkali feldspars ($Ab_{60.73}$, $An_{0.00}$, $Or_{39.27}$ in Ne-trachyte and $Ab_{72.26}$, $An_{0.00}$, $Or_{27.74}$ in Qz-trachyte) (Table 3). Aegerine is the main pyroxene type (average of 4.86% in nepheline trachyte and average of 1.61% in quartz trachyte) in addition to diopside with an averages of 3.42 and 0.89% in nepheline trachytes and quartz trachyte, respectively. Normative hypersthene is zero in nepheline trachyte while in quartz trachyte the average hypersthene content is 2.60 %.

The AHT exhibited leucocratic nature as indicated from the Differentiation Index (DI) of Thornton and Tuttle (1960) the differentiation index ranges from 84.04-88.7 in nepheline trachytes and from 87.59-91.15 in quartz trachytes. The studied samples are classified as trachyte according to Maitre *et al.* (1989) with a remarked affinity for the highly fractionated types toward rhyolite

Table 3: Some calculated indices and elemental ratios

	Ne-trachyte							Qz-trachyte					
Variabls	1	2	3	4	5	6	Average	7	8	9	10	11	Average
Feldspathoid saturation index	-0.18	-0.04	-0.13	-0.18	-0.16	-0.02	-0.12	9.58	15.41	11.80	14.02	21.21	14.40
Modified alkali-lime index	13.83	11.35	12.09	12.84	12.56	11.56	12.37	9.75	9.07	9.88	9.46	8.45	9.32
Aluminum saturation index	0.77	0.90	0.86	0.87	0.85	0.83	0.85	0.88	0.91	0.88	0.84	0.94	0.89
Agpaitic index	1.19	1.02	1.05	1.05	1.08	1.08	1.08	1.02	0.99	1.03	1.07	0.96	1.01
Differentiation index	84.04	88.02	87.93	88.70	87.05	85.98	86.95	89.78	90.02	90.82	87.59	91.15	89.87
Ab (%)	52.68	64.53	62.38	60.21	61.78	62.81	60.73	74.35	70.46	71.44	71.81	73.22	72.26
An (%)	0.00	0.00	0.00	0.00	0.00	0.00	0.00	0.00	0.00	0.00	0.00	0.00	0.00
Or (%)	47.32	35.47	37.62	39.79	38.22	37.19	39.27	25.65	29.54	28.56	28.19	26.78	27.74
Zr/Y	16.73	17.24	17.78	17.33	16.66	9.65	15.90	13.25	14.51	12.26	13.31	13.07	13.28
Zr/Ce	6.48	7.15	15.45	7.19	5.28	2.97	7.42	6.06	6.30	5.58	6.29	5.74	5.99
Zr/Rb	9.51	10.53	9.69	7.48	8.15	5.86	8.53	10.20	15.45	12.84	13.31	11.52	12.66
Zr/Nb	4.74	5.61	4.79	4.88	04.76	3.11	4.65	4.48	5.21	4.26	4.40	3.90	4.45

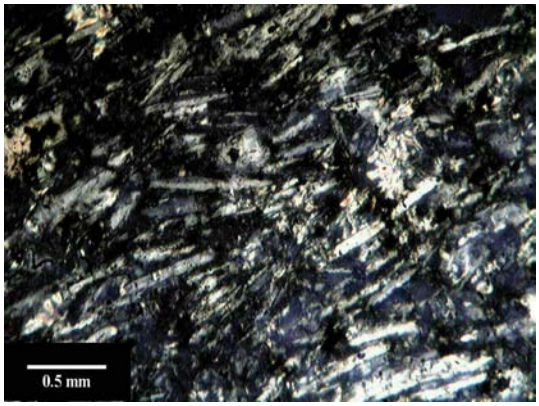

Fig. 2: Photomicrograph showing flow texture in AHT as the feldspar laths are arranged in a preferred orientation

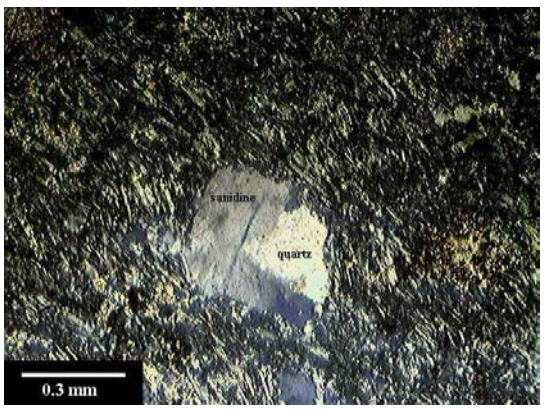

Fig. 3: Photomicrograph showing sanidine and quartz phenocrysts attacked by the quenched groundmass

field (Fig. 4) these rocks are alkaline according to Rickwood (1989) with a remarked orientation from the highly fractionated Qz-trachytes toward the subalkaline field. The AHT, plot within the field of continental oversaturated volcanics of Fitton (1987). Qz-trachytes plot in the Qz-normative field while the Ne-normative trachytes plot, mainly on or close to the margin between Qz-normative and Ne-normative rocks.

The present Ne-normative trachytes are slightly undersaturated based on Feldspathoid Silica-Saturation Index (FSSI) defined by Frost *et al.* (2001) as normative Q-(Lc+2(Ne+Kp))/100. Values of FSSI>0 indicate that the rock is silica-saturated and is undersaturated if FSSI<0. Accordingly, the present Ne-normative trachytes are slightly undersaturated as the average of FSSI is -0.12 while in Qz-normative trachytes the average of FSSI is 14.40 (Table 3).

The Ne-normative trachytes are shoshonitic according to Maitre *et al.* (1989) while the Qz-normative trachytes are high-K series (Fig. 5). The present trachytes are of peralkaline-meta-aluminous nature based on Agpaitic Index (AI) and Aluminum-Saturation Index (ASI), respectively. The later is expressed by molecular Al/(Ca-1.67P+Na+K) Shand (1947) and Zen (1988) all samples are meta-aluminous as the ASI values are <1, (average ASI = 0.85 and 0.89 for Ne-trachytes and Qz-trachytes, respectively (Table 3). The agpaitic index (AI = Na+K/Al mol%) reveals a peralkaline nature for AHT as the average agpaitic indices in Ne-trachytes and Qz-trachyes are 1.08, 1.01, respectively with a remarked orientation from the highly fractionated quartz trachytes toward the alkaline field (Fig. 6).

The values of the Modified Alkali-Lime Index (MALI) are closely related to the fractionation trends of the mineral assemblages that have crystallized and extracted from their parent melts, Frost *et al.* (2001). Figure 7 shown the relation between Modified Alkali Lime Index (MALI) and the SiO_2 contents in various mineral assemblages (Frost and Frost, 2008) AHT plot in the alkali field and are characterized by high MALI values as the minerals that contribute, essentially to produce such high MALI values are K-feldspar and albite while anorthite

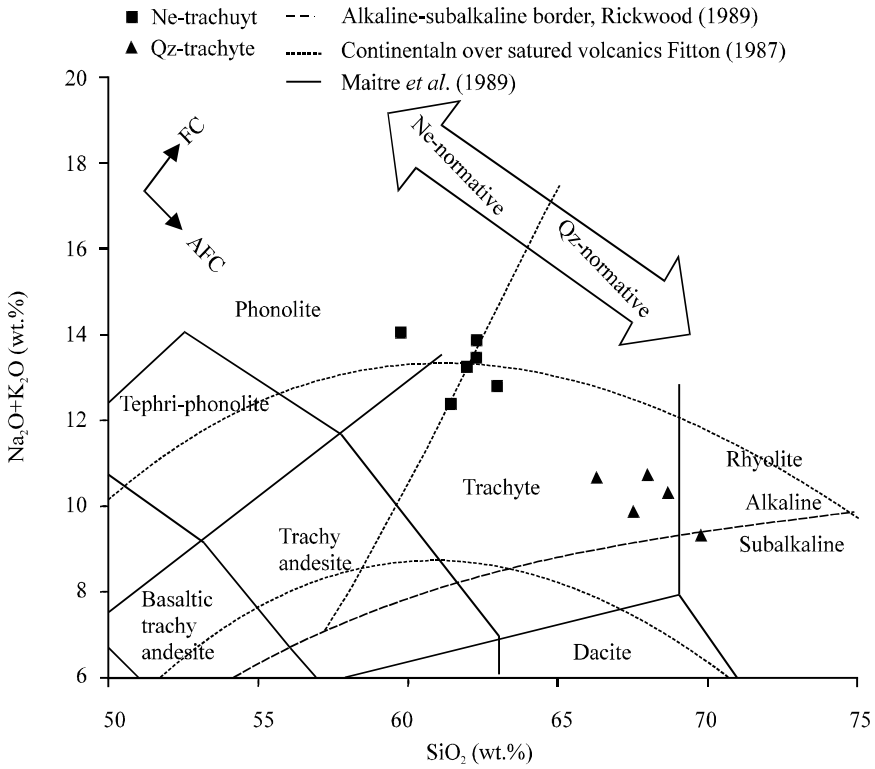

Fig. 4: Total alkali silica diagram for the studied trachytes the heavy dashed line of Rickwood (1989) separates between subalkaline and alkaline fields the dash-dot line separates Ne-normative and Qz-normative fields the area between the dashed lines represent the continental oversaturated volcanics (Fitton, 1987) the solid lines represent the chemical classification fields, after Maitre *et al.* (1989) the vectors pointing out to the trends of Fractional Crystallization (FC) and Assimilation Fractional Crystallization (AFC). The AHT plot mainly in the alkaline field with a dominant orientation of the highly fractionated Qz-trachyte samples towards the sub-alkaline-rhyolite field indicating a dominant role of AFC

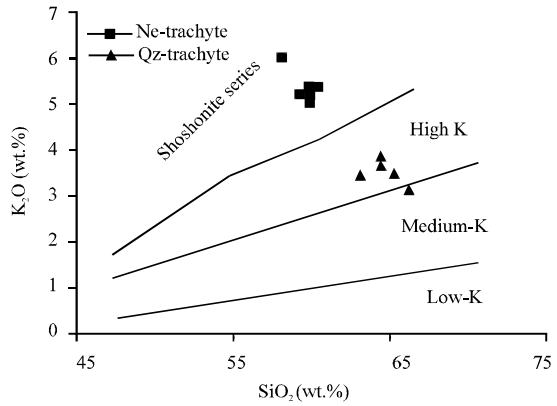

Fig. 5: SiO_2 versus K2O, fields after Maitre *et al.* (1989) the Ne-trachyte samples plot in the shoshonite series field while Qz-trachyte samples plot in the high K-field and fractionate toward medium-K calc-alkaline field

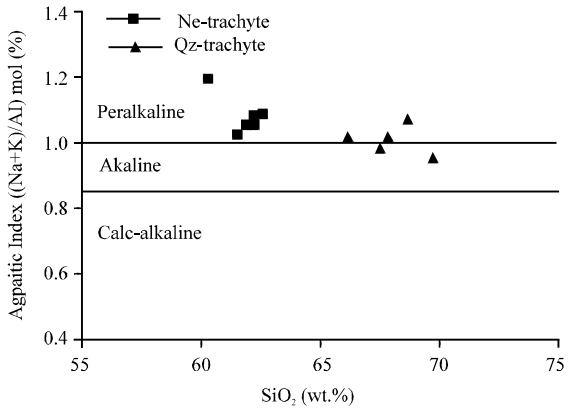

Fig. 6: SiO_2 versus agpaitic index showing an over all peralkaline affinity for the AHT, all Ne-trachytes and most of Qz-trachytes samples have agpaitic index >1 and plot within peralkaline field, except for two Qz-trachyte samples of agpaitic index between 0.87 and 1, plot in the alkaline field

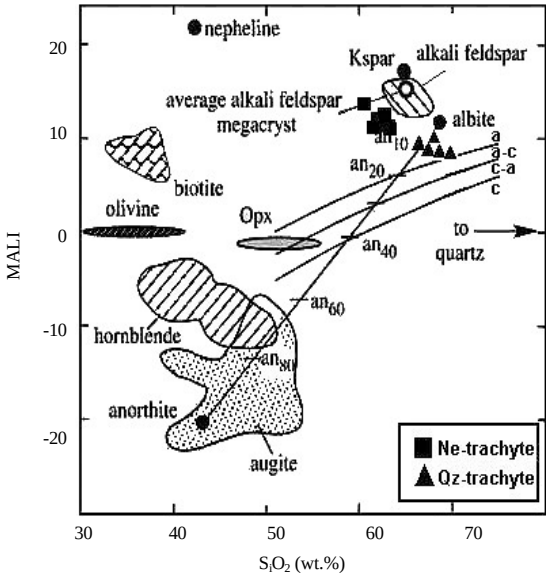

Fig. 7: SiO_2 versus Modified Alkali Lime Index (MALI) the three solid curved lines separate fields c: calcic; c-a: calcic alkali; a-c: alkali calcic and a: alkalic, Frost *et al.* (2001). The mineral assemblages presented are from Frost and Frost (2008). The AHT characterized by high MALI values and plot in the alkali field

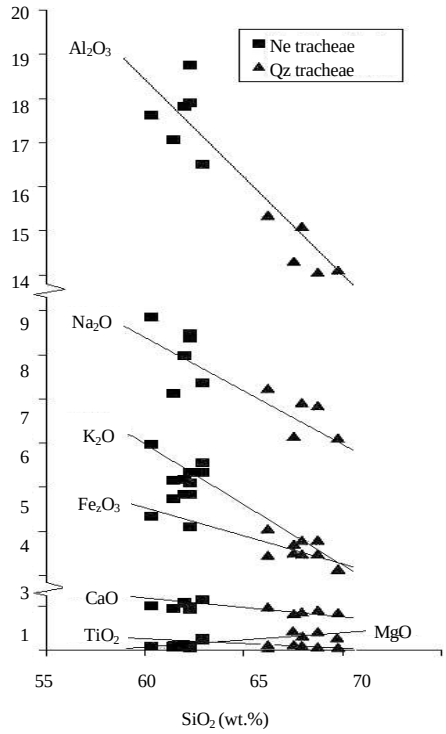

Fig. 8: SiO_2 versus major oxides

contribution is <10% fractionation. The studied AHT show a limited range of geochemical variations but such variations are to great extent far from random, Al_2O_3, CaO, Na_2O and K_2O correlate negatively with the increasing SiO_2 contents while MgO correlates positively towards the more fractionated Qz-trachytes (Fig. 8) this may reflect a pronounced role of Assimilation Fractional Crystallization (ACF) led to evolution of Qz-trachyte series. A lack of differentiation interval observed at S_iO_2 content between 63 and 66%, may be due to a process of rapid differentiation at that interval, White *et al.* (2009). The incompatible trace elements (Nb, La, Ce, Y and Zr) correlate positively with increasing silica contents, indicating a dominant role of fractional crystallization. The fractional crystallization proceeds until a certain SiO_2 content is reached then the positive correlation trends inverted to negative correlation during the evolution of Qz-trachytes such reversal in fractionation trends refers to processes of Assimilation Fractional Crystallization (AFC) (Fig. 9). Yttrium, Zr, Nb, La and Ce exhibit parabolic trends as the positive correlation trends inverted to negative correlation at S_iO_2 content = 67.5%, versus Y = 198 ppm, Zr = 2837 ppm, Nb = 551 ppm, La = 308 ppm and Ce = 456 ppm. The same feature is also noticed for some transition elements such as Co and Cu. The large ion lithophile elements (Ba and Sr) exhibit negative correlation trends with increasing of SiO_2 content. Th, Rb and Zn don't attain coherent trends between Ne-trachytes and the more evolved Qz-trachytes with increasing of SiO_2 content, however in Qz-trachyte phase the three elements decrease drastically towards the highly fractionated Qz-trachytes (Fig. 9).

The incompatible (immobile) elements (Y, Nb, Ce and Rb) show positive trends when correlated with Zr as a fractionation index (Fig. 10) these trends are more kin to fractional crystallization rather than assimilation fractional crystallization such coherent relations reflect the major roll of zircon, Davies and Macdonald (1987). Zr/Y and Zr/Ce ratios are relatively high and nearly constant between Ne-trachyte and Qz-trachyte with an average of 15.9 and 7.42, respectively indicating a within plate enrichment source. Zr/Rb ratio varies between Ne- trachytes and Qz-trachytes (8.53 and 12.66 in average, respectively) while the Zr/Nb ratio remains more or less constant between Ne-trachytes and Qz-trachytes (4.65-4.45 in average, respectively) indicating a very restricted role of crustal contamination during the differentiation of the residual parent melts (Macdonald *et al.*, 1987).

Transition elements usefully complement that of the Rare Earth Elements (REEs), since they are

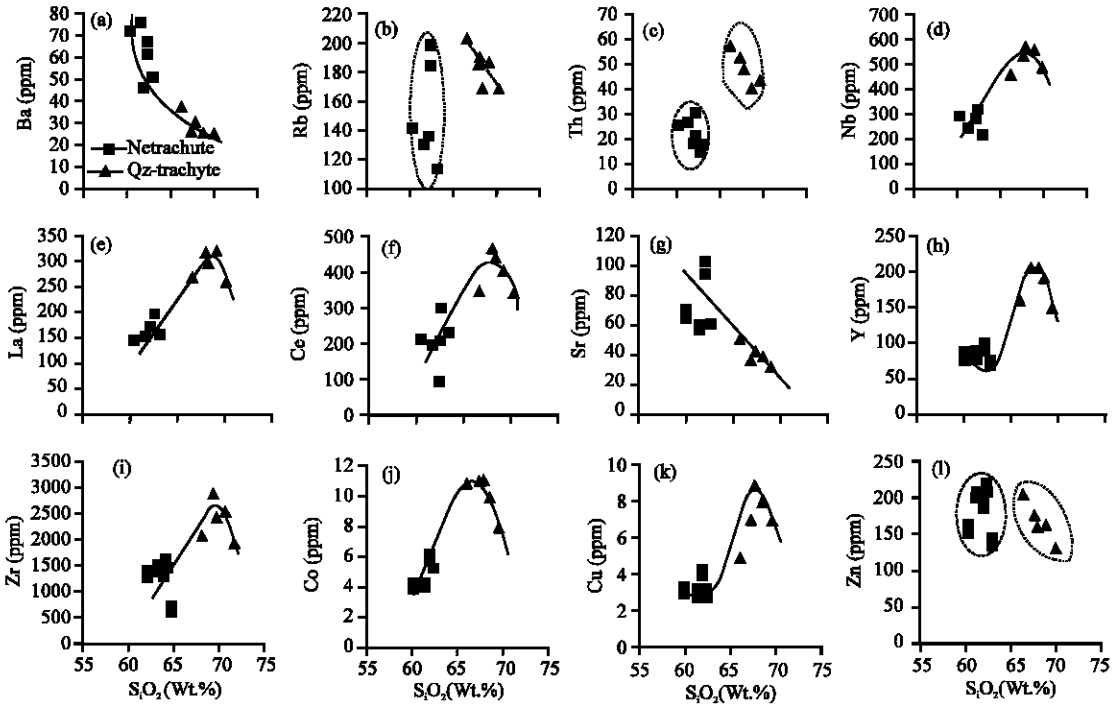

Fig. 9: a-l) SiO_2 versus trace elements

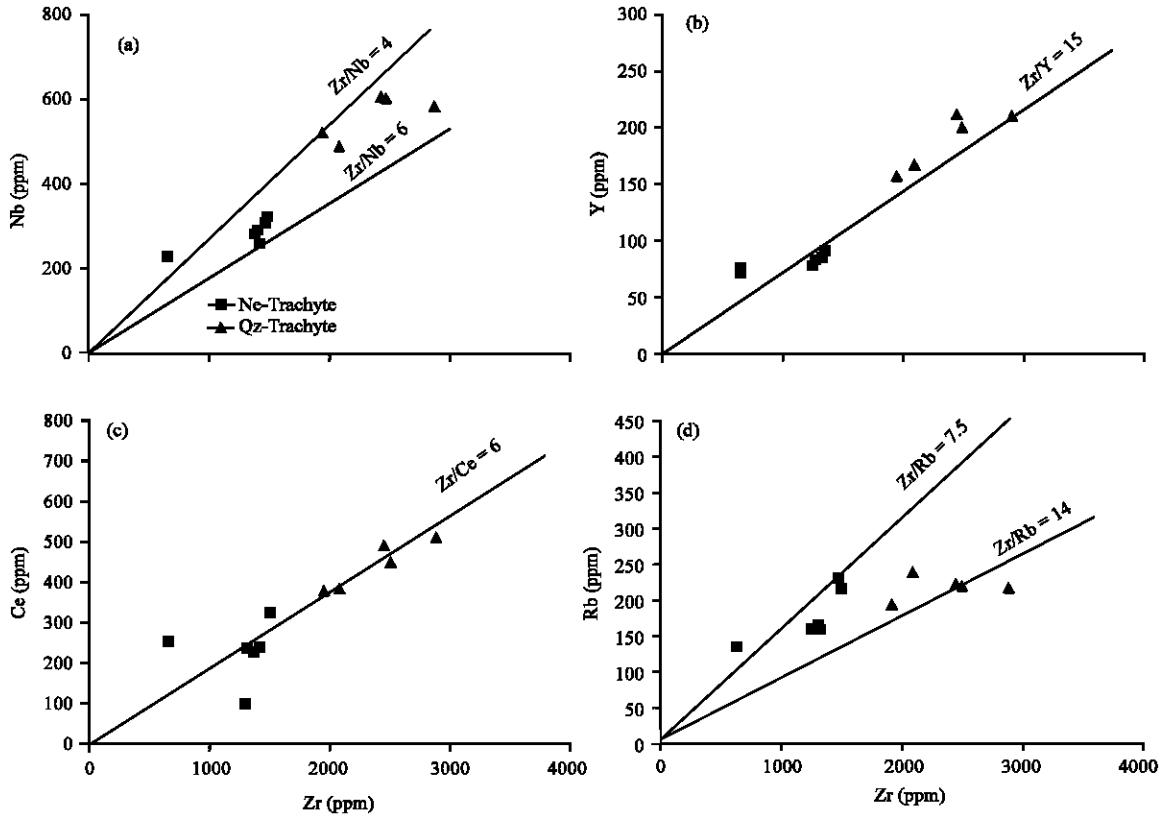

Fig. 10: a-d) Zr versus Nb, Y, Ce and Rb

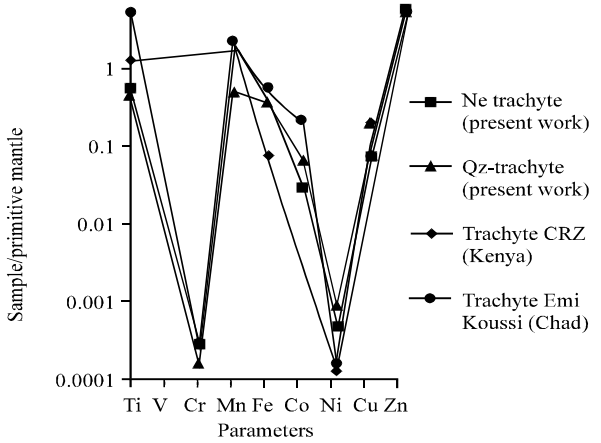

Fig. 11: Primitive mantle normalized transition elements for AHT, normalization values are after Sun (1982), compared with trachytes from Central Rift Zone (CRZ) of Kenya and trachytes from Emi Koussi Chad

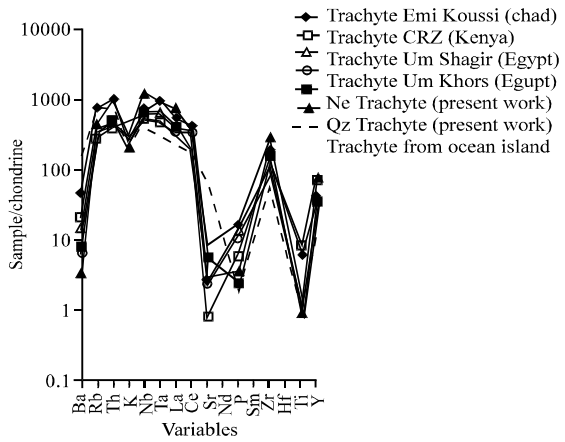

Fig. 12: Chondrite normalized incompatible elements for AHT, normalization values are after Thompson (1982), correlated with trachytes from; Kenya Continental Rift Zone (CRZ), trachytes from Emi Koussi Chad, Trachyte from Um Khors and Um Shaghir, Egypt and trachytes from Tristan de Cunha ocean Island

concentrated in the mafic solid phases and become impoverished in residual melts. All'egre has used Sc-Zn series spider diagram (Fig. 11). In this Fig. 11, the elements are normalized to primitive mantle values, Sun, (1982) and compared with trachytes from Central Rift Zone (CRZ) of Kenya (Price *et al.* (1985) and trachytes from Emi Koussi Chad (Gourgaud and Vincent, 2004). The resultant patterns attain characteristic troughs at Cr and Ni through the increase of the differentiation. It is also clear that the present trachyte patterns are close to that of East African rift trachytes with a lesser degree of fractionation.

Since, the tectonic setting of the trachytic rocks are usually restricted to within plate tectonic regimes. The studied samples are normalized to chondritic values of Thompson (1982) and correlated with trachytes from; Kenya Continental Rift Zone (CRZ) (Baker *et al*., 1977, 1964) trachytes from Emi Koussi Chad (Gourgaud and Vincent, 2004) trachyte from Um Khors and Um Shaghir, Egypt (Gharib *et al*., 2012) and trachyte from Tristan de Cunha ocean Island (Barker *et al*., 1984) (Fig. 12). The resulted patterns exhibit strong correlation between Egyptian trachytes (Abu Hibban, Um Khors and Um Shaghir) with that evolved from the East African rift. The present trachyte is enriched in immobile Zr, Y, P and Ti and depleted in mobile elements Sr, Ba, Rb and K with respect to that formed within oceanic plate. Such variations reflect the role of the subcontinental lithospheric mantle as a source of enrichment.

Application of AHT as a flux in ceramic industries: Figure 13 exhibits the melting behaviour of the

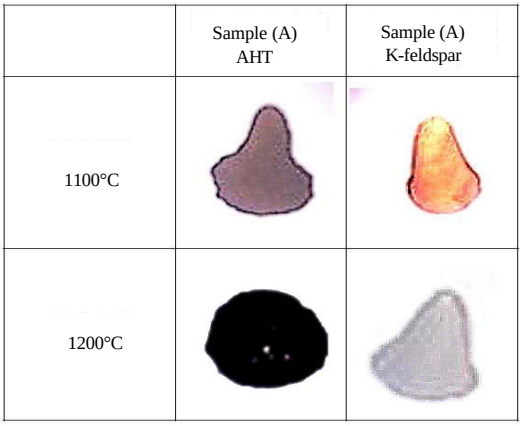

Fig. 13: Melting behavior of the representative trachyte cone samples (A) after firing for 1 h at 1100 and 1200°C as compared with K-feldspar (B)

representative trachyte cone samples after firing for 1 h at 1100 and 1200°C as compared with those of the K-feldspar samples. The XRD patterns of the fired samples are shown in (Fig. 14). It is clear that, on firing at 1100°C trachyte shows the densification by liquid phase, i.e., verification as seen in its larger rounded base as compared with that of K-feldspar. The residual crystalline phases, coexisted in both of the vitrified trachyte and K-feldspar samples are anorthoclase, quartz and hematite with relatively higher quartz and lower hematite in the later sample. On raising the firing temperature up to 1200°C the

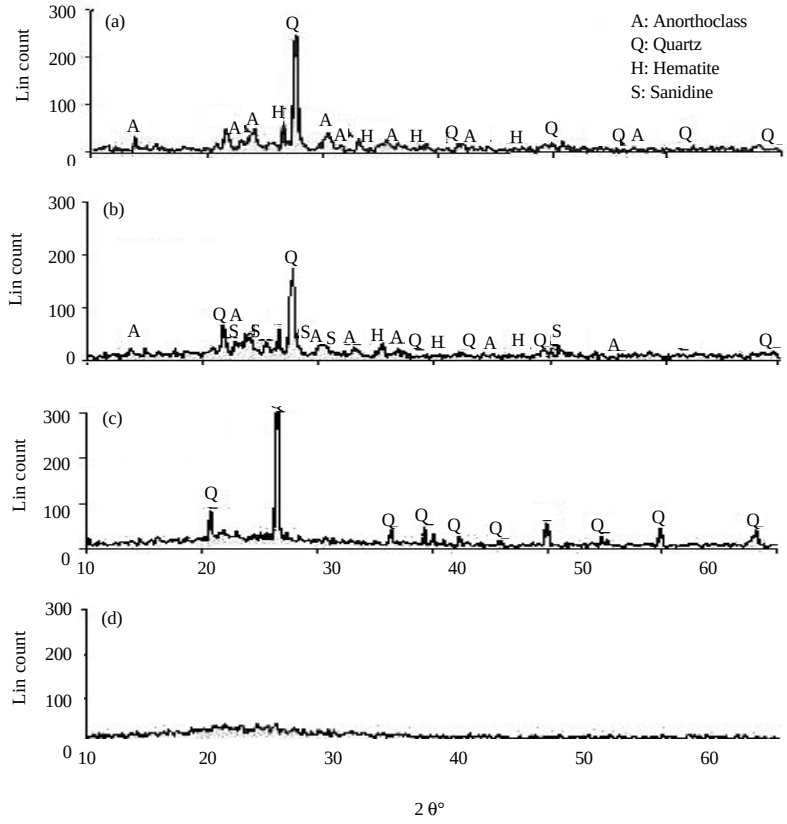

Fig. 14: XRD patterns of the powders representative trachyte samples after firing for 1 h at 1100 and 1200°C as compared with K-feldspar: a) K-feldspar1100°C; b) Trachyte 1100°C; c) K-feldspar 1200°C; d) Trachyte1200°C

trachyte sample is almost completely fused, giving only silicate glassy phase whereas the K-feldspar one is partly melted with only low quartz phase coexisting within the glassy phase.

CONCLUSION

The present AHT exhibited a remarked mineralogical and geochemical alkaline-peralkaline nature. The Agpaitic Index (AI) varies from 1.02-1.19 in nepheline normative trachytes and from 0.96-1.03 in quartz normative trachytes, the Feldspathoid Silica Saturation Index (FSSI) varies from -0.18-0.02 in nepheline normative trachytes and from 11.80-15.41 in quartz normative trachytes. The Modified Alkali-Lime Index (MALI) ranges from 11.35-13.83 in nepheline normative trachytes and from 8.45-9.88 in quartz normative trachytes. The AHT are meta-aluminous as the Aluminum Saturation Index (ASI) varies from 0.77-0.90 in nepheline normative trachytes and from 0.84-0.94 in quartz normative trachytes.

The fractionation trends of AHT revealed that the nepheline normative trachytes were derived as a result of fractional crystallization processes from more basic saturated to undersaturated magma and prior to fractionation of quartz trachytes the residual melts subjected to crustal contamination giving rise to processes of assimilation fractional crystallization led to the production of the more evolved quartz normative trachytes.

Variation patterns between major oxides revealed that Na_2O and K_2O correlate negatively with increasing SiO_2 contents such patterns of differentiation reflect the role of assimilation fractional crystallization. The assimilation fractional crystallization is thought to be initialized at SiO_2 content = 67.5 %, versus to Y = 198 ppm, Zr = 2837 ppm, Nb = 551 ppm, La = 308 ppm and Ce = 456 ppm.

The continuation of assimilation fractional crystallization processes affected the nature of the parental melts from per-alkaline to alkaline moreover the highly fractionated quartz trachyte trends were oriented toward the calc-alkaline medium-K-series.

The incompatible (immobile) elements (e.g., Y, Nb, Ce) show positive differentiation trends more kin to fractional crystallization than assimilation fractional crystallization,

when correlated with Zr as a fractionation index such coherent relations reflect the major role of zircon. The Zr/Nb ratio is more or less constant between nepheline normative trachyte and quartz normative trachytes (4.65 and 4.45, respectively).

The AHT were erupted within continental plate and characterized by enrichment of immobile elements; Zr, Y, P and Ti and depleted in mobile elements; Sr, Ba, Rb and K with respect to that formed within oceanic plates. Such variations between the two suites reflect the role of the subcontinental lithosphere in the continental rift zones.

The AHT characterized by favorable mineralogical and chemical characteristics, efficient to partially or completely replace K-feldspars in ceramic mixtures as a flux. The representative average sample of AHT (mixture of normative quartz trachyte and normative nepheline trachyte 1:1 weight ratio) has melting point lesser than K-feldspar and forms a completely liquid phase on firing at 1200°C.

REFERENCES

Aly, M.H. and B.N. Shalaby, 2001. Geochemical characterization of trachytic rocks for stoneware recipes: An example on Abu Khruq trachytic plugs, Eastern Desert, Egypt. Bull. NRC. Egypt, 26: 303-319.

Baker, B.H., G.G. Goles, W.P. Leeman and M.M. Lindstrom, 1977. Geochemistry and petrogenesis of a basalt-benmoreite-trachyte suite from the southern part of the Gregory Rift, Kenya. Contrib. Mineral. Petrol., 64: 303-332.

Baker, P.E., I.G. Gass, P.G. Harris and L.R.W. Maitre, 1964. The volcanological report of the royal society expedition to Tristan da Cunha, 1962. Philos. Trans. Royal Soc. London Math. Phys. Eng. Sci., 256: 439-575.

Davies, G.R. and R. Macdonald, 1987. Crustal influences in the petrogenesis of the naivasha basalt-comendite complex: Combined trace element and Sr-Nd-Pb isotope constraints. J. Petrol., 28: 1009-1031.

Dawood, Y.H., E.H.A. Naby and A.A. Sharafeldin, 2004. Influence of the alteration processes on the origin of uranium and europium anomalies in trachyte, central Eastern Desert, Egypt. J. Geochem. Explor., 81: 15-27.

Esposito, L., A. Salem, A. Tucci, A. Gualtieri and S.H. Jazayeri, 2005. The use of nepheline-syenite in a body mix for porcelain stoneware tiles. Ceram. Int., 31: 233-240.

Fitton, J.G., 1987. The cameroon line, West Africa: A comparison between oceanic and continental alkaline volcanism. Geol. Soc. London Spec. Publ., 30: 273-291.

Frost, B.R. and C.D. Frost, 2008. A geochemical classification for feldspathic igneous rocks. J. Petrol., 49: 1955-1969.

Frost, B.R., C.G. Barnes, W.J. Collins, R.J. Arculus and D.J. Ellis et al., 2001. A geochemical classification for granitic rocks. J. Petrol., 42: 2033-2048.

Gaied, M.E. and W. Gallala, 2015. Beneficiation of feldspar ore for application in the ceramic industry: Influence of composition on the physical characteristics. Arabian J. Chem., 8: 186-190.

Gharib, M.E., M.A. Obeid and A.H. Ahmed, 2012. Paleozoic alkaline volcanism: Geochemistry and petrogenesis of Um Khors and Um Shaghir trachytes of the central Eastern Desert, Egypt. Arabian J. Geosci., 5: 53-71.

Gourgaud, A. and P.M. Vincent, 2004. Petrology of two continental alkaline intraplate series at Emi Koussi volcano, Tibesti, Chad. J. Volcanol. Geotherm. Res., 129: 261-290.

Hashad, A.H., M.A. Hassan and A.A.A. Gadayel, 1978. Trace element variations in the alkaline volcanics of Wadi Natash, Egypt. Bull. Fac. Sci. KSA., 2: 195-204.

Hashad, M.H., 1994. Geochemical characterization and petrogenesis of phonolite-trachyte plugs associated with Wadi Natash volcanic rocks. Middle East Res. Centre Ain Shams Univ. Earth Sci. Ser., 8: 131-145.

Kunduraci, N. and T. Aydin, 2015. The effect of nepheline syenite addition on sanitary ware body. Int. J. Eng. Res. Dev., 7: 16-19.

Macdonald, R., G.R. Davies, C.M. Bliss, P.T. Leat and D.K. Bailey *et al*., 1987. Geochemistry of high-silica peralkaline rhyolites, Naivasha, Kenya Rift Valley. J. Petrol., 28: 979-1008.

Maitre, L.R.W., P. Bateman, A. Dudek, J.L. Keller and M.J. LeBase *et al*., 1989. A Classification of Igneous Rocks and Glossary of Terms. Blackwell, Oxford, England, ISBN: 9780632025930, Pages: 193.

Meneisy, M.Y., 1986. Mesozoic igneous activity in Egypt. Qatar Univ. Sci. Bull., 6: 317-328.

Moghazi, A.M., M.A. Hassanen and F.H. Mohamed, 1997. Source and evolution history of some mesozoic alkaline volcanics in the Eastern Desert of Egypt: Inference from petrology and geochemistry. J. Afr. Earth Sci., 24: 11-28.

Mohamed, F.H., 1998. Geochemistry and petrogenesis of El Gezira ring complex, Egypt: A monzosyenite cumulate derived from fractional crystallization of trachyandesitic magma. J. Volcanol. Geotherm. Res., 84: 103-123.

Mohamed, F.H., 2001. The natash alkaline volcanic field, Egypt: geochemical and mineralogical inferences on the evolution of a basalt to rhyolite eruptive suite. J. Volcanol. Geotherm. Res., 105: 291-322.

Price, R.C., R.W. Johnson, C.M. Gray and F.A. Frey, 1985. Geochemistry of phonolites and trachytes from the summit region of Mt. Kenya. Contrib. Mineral. Petrol., 89: 394-409.

Rickwood, P.C., 1989. Boundary lines within petrologic diagrams which use oxides of major and minor elements. Lithos, 22: 247-263.

Ryan, W. and C. Radford, 1987. Whitewares Production, Testing and Quality Control: Including Materials, Body Formulations and Manufacturing Processes. Pergamon Press, Pergamon, Turkey, ISBN: 9780080349275, Pages: 333.

Shand, S.J., 1947. The Eruptive Rocks. 3rd Edn., John Wiley and Sons, New York, USA., Pages: 444.

Sun, S.S., 1982. Chemical composition and origin of the earths primitive mantle. Geochim. Cosmochim. Acta, 46: 179-192.

Thompson, R.N., 1982. Magmatism of the British Tertiary volcanic province. Scott. J. Geol., 18: 49-107.

Thornton, C.P. and O.F. Tuttle, 1960. Chemistry of igneous rocks Part 1, Differentiation index. Am. J. Sci., 258: 664-684.

White, J.C., D.F. Parker and M. Ren, 2009. The origin of trachyte and pantellerite from Pantelleria, Italy: Insights from major element, trace element and thermodynamic modelling. J. Volcanol. Geotherm. Res., 179: 33-55.

Zen, E.A., 1988. Phase relations of peraluminous granitic rocks and their petrogenetic implications. Ann. Rev. Earth Planet. Sci., 16: 21-52.